Validation of global land-ocean aerosol products retrieved from the DPC-2/GF-5(02) on-orbit measurements

Zihan Zhang [1], Zhengqiang Li [1,2,3,*]

[1] Aerospace Information Research Institute, Chinese Academy of Sciences, Beijing 100101, China
[2] State Key Laboratory of Spatial Datum, College of Remote Sensing and Geoinformatics Engineering, Faculty of Geographical Science and Engineering, Henan University, Zhengzhou 450046, China
[3] University of Chinese Academy of Sciences, Beijing 100049, China

Keywords: Aerosol, Directional Polarization Camera (DPC), Polarization, Optimal Estimation.

Abstract

The Chinese second-generation Directional Polarization Camera (DPC-2) onboard the GF-5(02) satellite provides global multi-angle, multispectral polarization observations, effectively bridging the gap between POLDER/PARASOL and SPEXone/PACE. Using one year of DPC-2/GF-5(02) measurements, land-ocean aerosol products are generated by fully exploiting polarization and angular information to enhance sensitivity to aerosol properties. Ground-based observations from the AErosol RObotic NETwork (AERONET) are used to evaluate the retrieval accuracy of Aerosol Optical Depth at 550 nm (AOD_{550}), Ångström Exponent between 440 nm and 670 nm ($AE_{440\text{-}670}$), and Single Scattering Albedo at 440 nm (SSA_{440}), demonstrating the stability and reliability of the retrievals. For AOD_{550}, the Root Mean Square Error (RMSE) and bias are 0.109 and -0.006 over land, and 0.071 and -0.001 over ocean. For $AE_{440\text{-}670}$, the RMSE and bias are 0.488 and -0.151 over land, and 0.275 and -0.047 over ocean. For SSA_{440}, the RMSE and bias are 0.044 and 0.003 over land, and 0.039 and 0.002 over ocean. Comparisons with mainstream satellite aerosol products indicate comparable and consistent accuracy. Overall, these results provide a coherent global characterization of aerosol distribution and properties, highlighting the strong potential of DPC-2/GF-5(02) for long-term aerosol monitoring and climate research.

1. Introduction

The Intergovernmental Panel on Climate Change (IPCC) Sixth Assessment Report highlights aerosols as one of the most uncertain yet influential factors in the climate system (Pirani et al., 2024). Aerosols affect radiation balance and cloud processes, but their strong spatial and temporal variability poses major difficulties for accurate satellite retrieval (Liu et al., 2026; Zhang et al., 2023b; Zhang et al., 2025b).

Among satellite techniques, Multi-Angle Polarimeters (MAPs) show great promise in reducing aerosol retrieval uncertainties (Kokhanovsky et al., 2010; Mishchenko and Travis, 1997). Table 1 summarizes the long history of Chinese polarimeter development, including Synchronization Monitoring Atmosphere Corrector (SMAC) (Li et al., 2022b), Polarized Scanning Atmospheric Corrector (PSAC) (Li et al., 2022c), Directional Polarimetric Camera (DPC) series (Cheng et al., 2011; Li et al., 2022a; Li et al., 2018; Tu et al., 2025; Xie et al., 2025), and Particulate Observing Scanning Polarization (POSP) series (Ji et al., 2025b), and Polarized Multi-Angle Imager (PMAI) (Zhang et al., 2023a). The DPC-2 onboard Chinese GF-5(02) satellite enables multi-angle and multi-spectral polarimetric observations in several bands and effectively bridges the gap between POLDER/PARASOL (Fu and Hasekamp, 2018; Hasekamp et al., 2011) and SPEXone/PACE (Fu et al., 2025; Hasekamp et al., 2019) in global MAP observations (Li et al., 2022a).

Sensor	Satellite	Launch Time
DPC-1	GF-5	May 2018
SMAC	GFDM	July 2020
PSAC	HJ-2A/B	September 2020
DPC-2 & POSP-1	GF-5(02)	September 2021
DPC-3 & POSP-2	DQ-1	April 2022
DPC-4	TECIS-1	August 2022
PMAI	FY-3G	April 2023

Table 1. History of Chinese polarimeters.

Although several related studies exist, we have made first attempt to generate global aerosol products separately over land (Zhang et al., 2025a) and ocean (Ji et al., 2025a) using the Remote-sensing of Trace-gas and Aerosol Products (RemoTAP) algorithm. In this study, we integrated the land and ocean aerosol products into a unified global product and performed both quantitative and qualitative validations to assess overall accuracy.

2. Methodology

2.1 Aerosol retrieval algorithm

We apply the RemoTAP algorithm (Fu and Hasekamp, 2018; Fu et al., 2025; Hasekamp et al., 2011) for aerosol retrieval, as shown in Figure 1. The satellite measurements serve as inputs to generate the first guess of the state vector. The forward model then computes the Top-of-Atmosphere (ToA) results based on this state vector. It consists of both surface and atmospheric models for intermediate calculations, and employs the LINTRAN code (Schepers et al., 2014) to integrate the layer-by-layer physical parameters. If convergence is not achieved, the state vector is updated, and the iteration proceeds using a damped Gauss-Newton method with Phillips-Tikhonov regularization. Once convergence is reached, the final retrieval results are produced. The algorithm is described in detail by Lu et al. (2022).

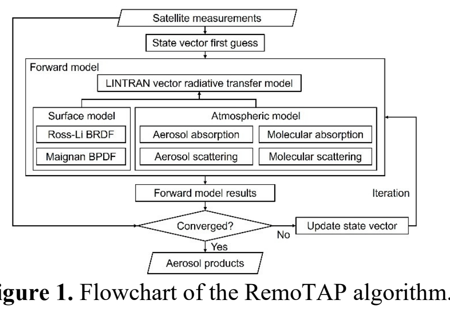

Figure 1. Flowchart of the RemoTAP algorithm.

The DPC-2/GF-5(02) satellite succeeds POLDER-2/PARASOL and DPC-1/GF-5, as shown in Figure 2. This on-orbit sensor provides reliable MAP observations with up to 17 viewing angles, ~3.3 km spatial resolution, and a 1,850 km swath. The polarization bands at 490 nm, 670 nm, and 865 nm, along with the radiance band at 565 nm, are used to generate aerosol products.

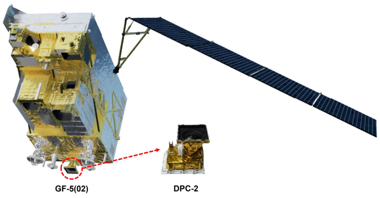

Figure 2. DPC-2/GF-5(02) sensor.

2.2 Validation approach

To evaluate the accuracy of aerosol retrievals, ground-based observations from the AErosol RObotic NETwork (AERONET) are used (Holben et al., 1998). Figure 3 shows the global distribution of AERONET sites used for validation. Only Level 2.0 data are employed to ensure validation quality, given the sufficient number of colocations. The AOD20 products are used for validating Aerosol Optical Depth (AOD) and Ångström Exponent (AE), while the INV20 products are used for validating Single Scattering Albedo (SSA). Quantitative validation is conducted by comparing the averaged satellite retrievals with ground-based observations within ±1 h (AOD, AE) or ±3 h (SSA) and a 20 km spatial radius around each site (Hasekamp et al., 2024).

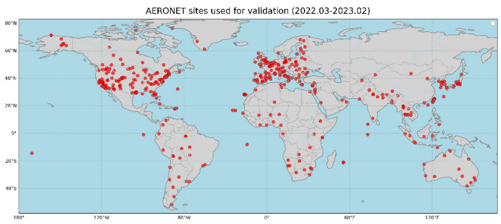

Figure 3. Global distribution of the referenced AERONET sites

Retrieval accuracy is evaluated using standard statistical metrics, including Mean Absolute Error (MAE), Root Mean Square Error (RMSE), bias, and STandard Deviation (STD). The Global Climate Observing System (GCOS) criteria serve as an additional benchmark, specifying target accuracies of max(0.04, 10%) for AOD and ±0.03 for SSA (Popp et al., 2016).

$$\mathrm{MAE} = \frac{\sum_{i=0}^{n}\left|x_{\mathrm{ret},n} - x_{\mathrm{anet},n}\right|}{n} \tag{1}$$

$$\mathrm{RMSE} = \sqrt{\frac{\sum_{i=0}^{n}\left(x_{\mathrm{ret},n} - x_{\mathrm{anet},n}\right)^2}{n}} \tag{2}$$

$$\mathrm{bias} = \frac{\sum_{i=0}^{n}\left(x_{\mathrm{ret},n} - x_{\mathrm{anet},n}\right)}{n} \tag{3}$$

$$\mathrm{STD} = \sqrt{\frac{\sum_{i=0}^{n}\left[\left(x_{\mathrm{ret},n} - x_{\mathrm{anet},n}\right) - \mathrm{bias}\right]^2}{n}} \tag{4}$$

where n is the number of colocations, $x_{\mathrm{ret},n}$ denotes the retrieved value, $x_{\mathrm{anet},n}$ denotes the corresponding AERONET value.

3. Results and Discussions

3.1 Quantitative validation

Quantitative validation is based on the ground-based AERONET observations. Aerosol products, including AOD, AE, and SSA, are validated against AERONET observations, as shown in Figure 4. The validation of AOD is performed at 550 nm, following the commonly adopted practice. To avoid spectral interpolation for ground-based observations, SSA is validated at 440 nm, and AE is validated using the 440 nm and 670 nm bands (Fu et al., 2025).

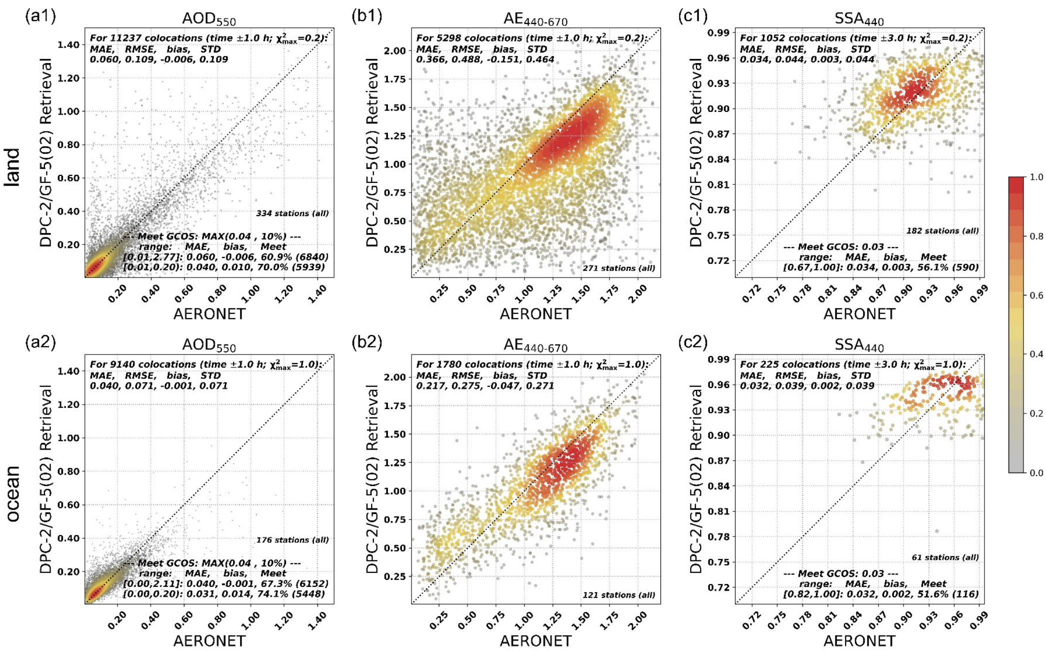

Figure 4. Validation of DPC-2/GF-5(02) aerosol products:
Rows (1) and (2) correspond to land and ocean retrievals, respectively; Columns (a), (b), and (c) show the validation scatterplots for AOD at 550 nm (AOD_{550}), AE between 440 nm and 670 nm ($AE_{440-670}$), and SSA at 440 nm (SSA_{440}), respectively.

In summary, these scatterplots indicate that the overall accuracy of aerosol retrievals over the ocean is higher than over land, which is attributed to the generally cleaner atmospheric conditions above the ocean. The comparison of DPC-2/GF-5(02) aerosol products with POLDER/PARASOL mainstream products (Hasekamp et al., 2024) is shown in Figure 5. It should be noted that the DPC-2/GF-5(02) and POLDER/PARASOL sensors do not have overlapping on-orbit periods; therefore, this comparison serves as a reference rather than a strict validation.

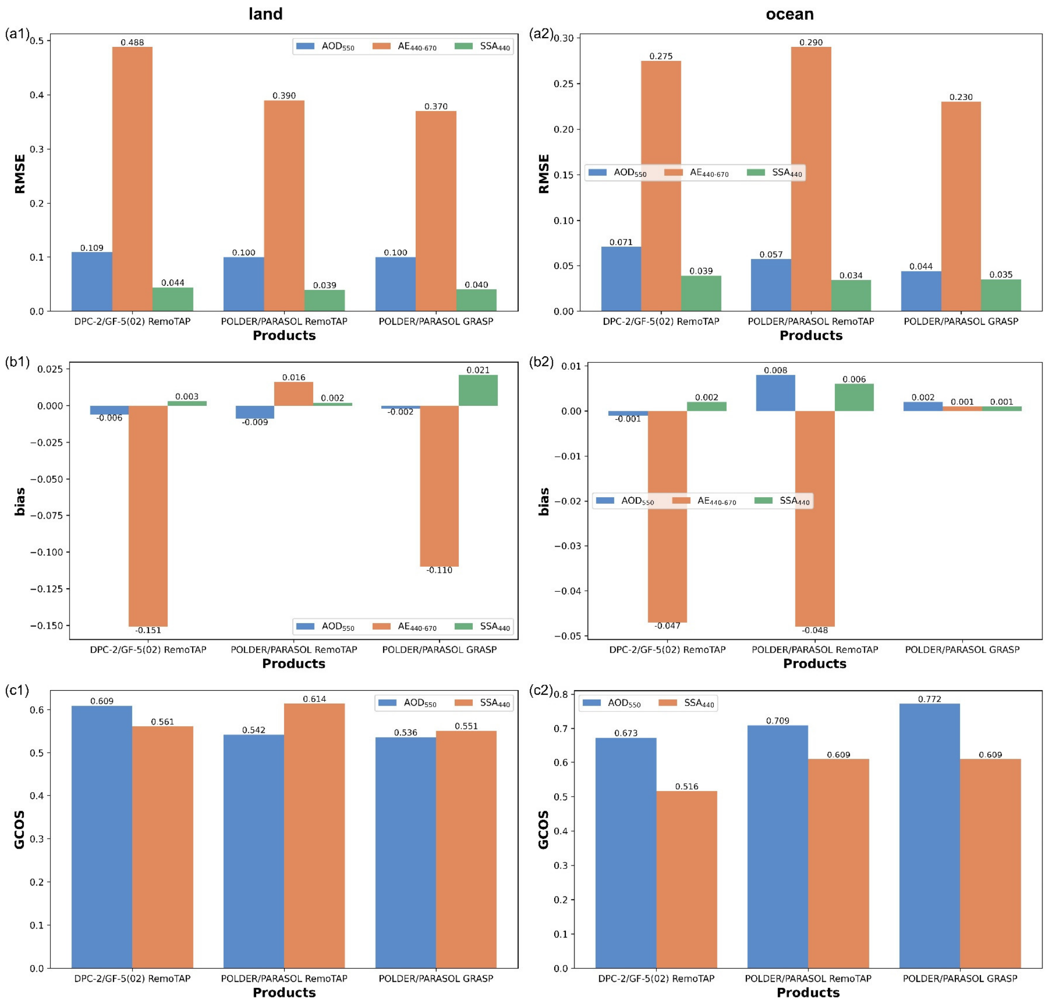

Figure 5. Comparison of DPC-2/GF-5(02) RemoTAP aerosol products with POLDER/PARASOL RemoTAP and GRASP products: Rows (a), (b), and (c) represent RMSE, bias, and GCOS statistics, respectively. Columns (1) and (2) correspond to retrievals over land and ocean, respectively. The blue, brown, and green bars indicate the accuracy for AOD_{550}, $AE_{440\text{-}670}$, and SSA_{440}, respectively.

For land and ocean retrievals, the DPC-2/GF-5(02) exhibits comparable RMSE values for AOD_{550}, $AE_{440\text{-}670}$, and SSA_{440} with both POLDER/PARASOL products, indicating stable and reliable performance in aerosol retrievals. The bias values of DPC-2/GF-5(02) remain generally small, although AE shows a slight tendency toward underestimation. Furthermore, the fraction of DPC-2/GF-5(02) AOD retrievals over land meeting the GCOS accuracy requirement reaches 60.9%, surpassing both POLDER/PARASOL products. For AE and SSA over land, as well as AOD, AE, and SSA over the ocean, the fractions meeting the GCOS criterion are generally comparable among these three products.

Overall, the DPC-2/GF-5(02) RemoTAP products exhibit strong consistency with mainstream MAP products, demonstrating high accuracy and reliability for global aerosol monitoring over both land and ocean.

3.2 Qualitative validation

Qualitative validation is conducted through global pattern analysis, illustrated by the annual mean distributions of aerosol products from May 2022 to February 2023 in Figure 6.

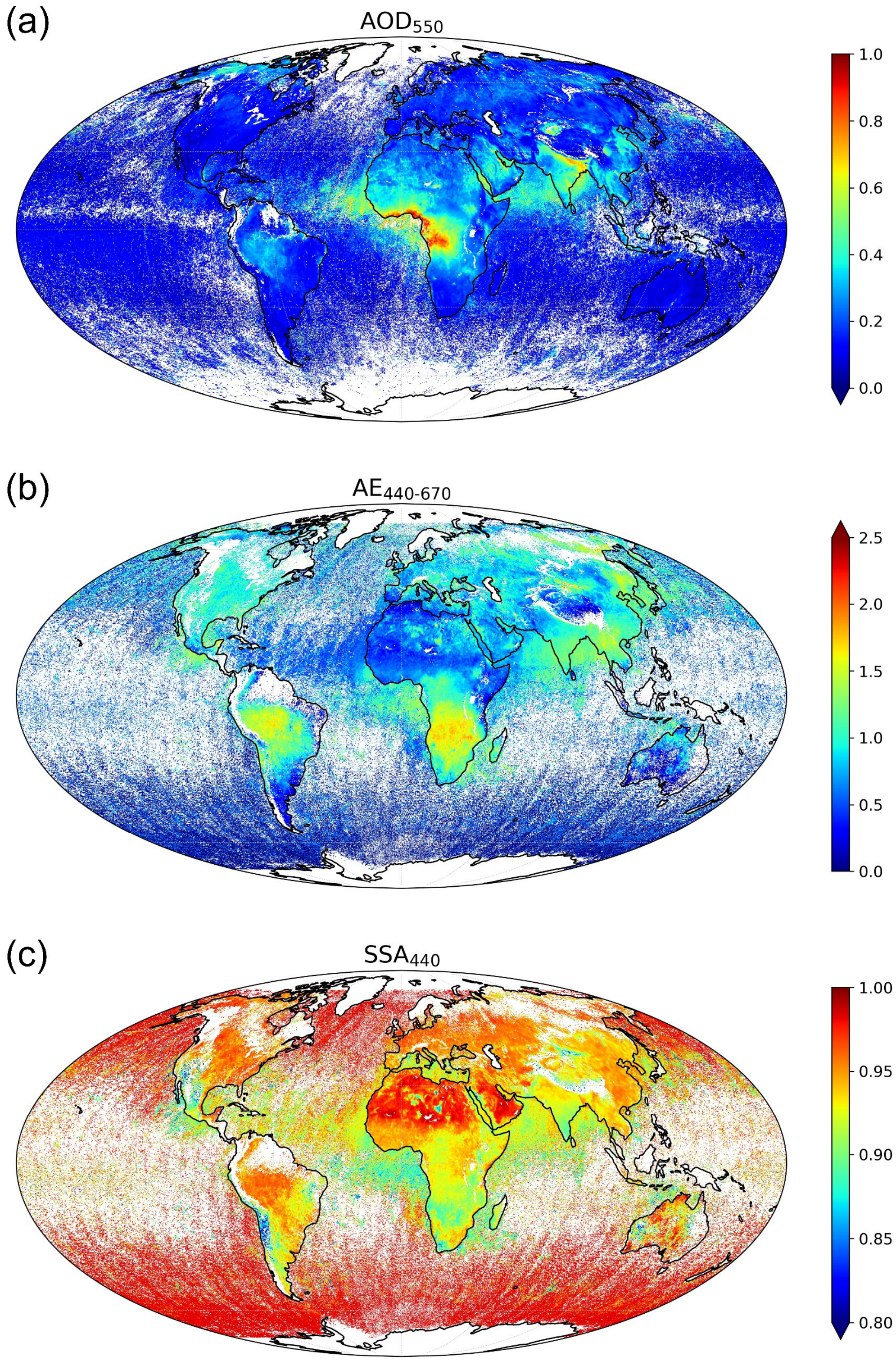

Figure 6. Global distributions of annual mean DPC-2/GF-5(02) aerosol products: (a) AOD_{550}, (b) $AE_{440\text{-}670}$, and (c) SSA_{440}.

As shown in the Figure 6, the global distributions of aerosol optical properties, including AOD_{550}, $AE_{440\text{-}670}$, and SSA_{440}, exhibit pronounced spatial variability and maintain consistent physical relationships.

The AOD represents the total aerosol loading, with high values observed mainly over northern North America, the Amazon, the Sahara, central Africa, the Arabian Peninsula, the Indian Peninsula, Southeast Asia, eastern coastal China, the Gulf of Guinea, the Arabian Sea, and the Bay of Bengal. Elevated AOD over the Sahara and the Arabian Peninsula is attributed to desert dust, whereas the high AOD over South and East Asia primarily arises from anthropogenic and industrial emissions. In contrast, oceanic regions exhibit low AOD, indicating relatively clean atmospheric conditions.

https://doi.org/10.5194/isprs-annals-XI-3-2026-989-2026

The AE, representing aerosol particle size, shows high values in regions dominated by fine-mode aerosols, such as areas affected by industrial emissions or biomass burning in North America, the Amazon, central Africa, South Asia, and East Asia. Conversely, low AE values are observed over the Sahara, Australia, and oceanic regions, indicating the predominance of coarse-mode dust and sea salt particles.

The SSA, which characterizes aerosol scattering properties, shows high values over oceanic and desert regions, consistent with predominantly scattering aerosols such as sea salt and dust. Lower SSA values are observed over southern Africa and Southeast Asia, indicating the presence of more absorbing aerosols, such as anthropogenic pollution or black carbon.

Overall, the global patterns of AOD, AE, and SSA are physically coherent and collectively reflect the spatial diversity of aerosol types across different regions.

4. Conclusions

Using the DPC-2/GF-5(02) satellite, this study presents the first global aerosol products over both land and ocean. Validation against AERONET observations and comparisons with POLDER/PARASOL products demonstrate the high accuracy and stability of the DPC-2/GF-5(02) retrievals. The global distributions of AOD, AE, and SSA effectively capture major aerosol sources while exhibiting physically consistent spatial patterns. Overall, DPC-2/GF-5(02) enhances international MAP observations and shows strong potential for long-term aerosol monitoring, offering valuable support for climate research. The global land-ocean aerosol products validated in this work are available at doi.org/10.57760/sciencedb.20859.

References

Cheng, T., Gu, X., Xie, D., Li, Z., Yu, T., Chen, X., 2011. Simultaneous retrieval of aerosol optical properties over the Pearl River Delta, China using multi-angular, multi-spectral, and polarized measurements. Remote Sensing of Environment, 115(7), 1643-1652.

Fu, G., Hasekamp, O., 2018. Retrieval of aerosol microphysical and optical properties over land using a multimode approach. Atmospheric Measurement Techniques, 11(12), 6627-6650.

Fu, G., Rietjens, J., Laasner, R., van der Schaaf, L., van Hees, R., Yuan, Z., van Diedenhoven, B., Hannadige, N., Landgraf, J., Smit, M., Knobelspiesse, K., Cairns, B., Gao, M., Franz, B., Werdell, J., Hasekamp, O., 2025. Aerosol Retrievals From SPEXone on the NASA PACE Mission: First Results and Validation. Geophysical Research Letters, 52(4), e2024GL113525.

Hasekamp, O., Litvinov, P., Fu, G., Chen, C., Dubovik, O., 2024. Algorithm evaluation for polarimetric remote sensing of atmospheric aerosols. Atmospheric Measurement Techniques, 17(5), 1497-1525.

Hasekamp, O.P., Fu, G., Rusli, S.P., Wu, L., Di Noia, A., Brugh, J.a.d., Landgraf, J., Martijn Smit, J., Rietjens, J., van Amerongen, A., 2019. Aerosol measurements by SPEXone on the NASA PACE mission: expected retrieval capabilities. Journal of Quantitative Spectroscopy and Radiative Transfer, 227, 170-184.

Hasekamp, O.P., Litvinov, P., Butz, A., 2011. Aerosol properties over the ocean from PARASOL multiangle photopolarimetric measurements. Journal of Geophysical Research: Atmospheres, 116(D14).

Holben, B.N., Eck, T.F., Slutsker, I., Tanré, D., Buis, J.P., Setzer, A., Vermote, E., Reagan, J.A., Kaufman, Y.J., Nakajima, T., Lavenu, F., Jankowiak, I., Smirnov, A., 1998. AERONET—A Federated Instrument Network and Data Archive for Aerosol Characterization. Remote Sensing of Environment, 66(1), 1-16.

Ji, Z., Li, Z., Zhang, Z., Fu, G., Hasekamp, O., Fan, C., Liu, Q., de Leeuw, G., 2025a. Retrieval of Aerosol Properties Over the Ocean Using Data From the Second-Generation Directional Polarization Camera (DPC-2) Onboard the GF-5(02) Satellite. Journal of Geophysical Research: Atmospheres, 130(17), e2025JD043908.

Ji, Z., Li, Z., Zhang, Z., Leeuw, G.d., Ma, Y., Shi, Z., 2025b. An Aerosol Retrieval Algorithm over Land from Multispectral Single-Viewing Measurements of Intensity and Polarization. IEEE Transactions on Geoscience and Remote Sensing, 63, 1-14.

Kokhanovsky, A.A., Deuzé, J.L., Diner, D.J., Dubovik, O., Ducos, F., Emde, C., Garay, M.J., Grainger, R.G., Heckel, A., Herman, M., Katsev, I.L., Keller, J., Levy, R., North, P.R.J., Prikhach, A.S., Rozanov, V.V., Sayer, A.M., Ota, Y., Tanré, D., Thomas, G.E., Zege, E.P., 2010. The inter-comparison of major satellite aerosol retrieval algorithms using simulated intensity and polarization characteristics of reflected light. Atmospheric Measurement Techniques, 3(4), 909-932.

Li, Z., Hou, W., Hong, J., Fan, C., Wei, Y., Liu, Z., Lei, X., Qiao, Y., Hasekamp, O.P., Fu, G., Wang, J., Dubovik, O., Qie, L., Zhang, Y., Xu, H., Xie, Y., Song, M., Zou, P., Luo, D., Wang, Y., Tu, B., 2022a. The polarization crossfire (PCF) sensor suite focusing on satellite remote sensing of fine particulate matter PM2.5 from space. Journal of Quantitative Spectroscopy and Radiative Transfer, 286, 108217.

Li, Z., Hou, W., Hong, J., Zheng, F., Luo, D., Wang, J., Gu, X., Qiao, Y., 2018. Directional Polarimetric Camera (DPC): Monitoring aerosol spectral optical properties over land from satellite observation. Journal of Quantitative Spectroscopy and Radiative Transfer, 218, 21-37.

Li, Z., Hou, W., Qiu, Z., Ge, B., Xie, Y., Hong, J., Ma, Y., Peng, Z., Fang, W., Zhang, D., Sun, X., Qiao, Y., Yu, J., Yang, W., Lin, J., Hu, Z., 2022b. Preliminary On-Orbit Performance Test of the First Polarimetric Synchronization Monitoring Atmospheric Corrector (SMAC) On-Board High-Spatial Resolution Satellite Gao Fen Duo Mo (GFDM). IEEE Transactions on Geoscience and Remote Sensing, 60, 1-14.

Li, Z., Xie, Y., Hou, W., Liu, Z., Bai, Z., Hong, J., Ma, Y., Huang, H., Lei, X., Sun, X., Liu, X., Yang, B., Qiao, Y., Zhu, J., Cong, Q., Zheng, Y., Song, M., Zou, P., Hu, Z., Lin, J., Fan, L., 2022c. In-Orbit Test of the Polarized Scanning Atmospheric Corrector (PSAC) Onboard Chinese Environmental Protection and Disaster Monitoring Satellite Constellation HJ-2 A/B. IEEE Transactions on Geoscience and Remote Sensing, 60, 1-17.

Liu, Q., Li, Z., Zhang, Z., Fu, G., Hasekamp, O., Li, L., Bai, Y., Fan, C., 2026. Polarized reflectance in China from DPC-2/GF-5(02) polarimetric satellite measurements: dataset and model inter-comparison. Journal of Quantitative Spectroscopy and Radiative Transfer, 360, 109961.

Lu, S., Landgraf, J., Fu, G., van Diedenhoven, B., Wu, L., Rusli, S.P., Hasekamp, O.P., 2022. Simultaneous Retrieval of Trace Gases, Aerosols, and Cirrus Using RemoTAP—The Global Orbit Ensemble Study for the CO2M Mission. Frontiers in Remote Sensing, 3.

Mishchenko, M.I., Travis, L.D., 1997. Satellite retrieval of aerosol properties over the ocean using polarization as well as intensity of reflected sunlight. Journal of Geophysical Research: Atmospheres, 102(D14), 16989-17013.

Pirani, A., Fuglestvedt, J.S., Byers, E., O’Neill, B., Riahi, K., Lee, J.-Y., Marotzke, J., Rose, S.K., Schaeffer, R., Tebaldi, C., 2024. Scenarios in IPCC assessments: lessons from AR6 and opportunities for AR7. npj Climate Action, 3(1), 1.

Popp, T., De Leeuw, G., Bingen, C., Brühl, C., Capelle, V., Chedin, A., Clarisse, L., Dubovik, O., Grainger, R., Griesfeller, J., Heckel, A., Kinne, S., Klüser, L., Kosmale, M., Kolmonen, P., Lelli, L., Litvinov, P., Mei, L., North, P., Pinnock, S., Povey, A., Robert, C., Schulz, M., Sogacheva, L., Stebel, K., Stein Zweers, D., Thomas, G., Tilstra, L.G., Vandenbussche, S., Veefkind, P., Vountas, M., Xue, Y., 2016. Development, Production and Evaluation of Aerosol Climate Data Records from European Satellite Observations (Aerosol_cci). Remote Sensing, 8(5), 421.

Schepers, D., aan de Brugh, J.M.J., Hahne, P., Butz, A., Hasekamp, O.P., Landgraf, J., 2014. LINTRAN v2.0: A linearised vector radiative transfer model for efficient simulation of satellite-born nadir-viewing reflection measurements of cloudy atmospheres. Journal of Quantitative Spectroscopy and Radiative Transfer, 149, 347-359.

Tu, B., Fan, L., Yao, P., Ti, R., Wang, Y., Yu, H., Xiang, G., Meng, B., Hong, J., 2025. An On-orbit parameter adjustment approach for DQ-1 Directional Polarimetric Camera based on the cloud data of MODIS/AUQA. Journal of Quantitative Spectroscopy and Radiative Transfer, 345, 109582.

Xie, D., Guo, L., Wu, Y., Chen, Q., Zuo, X., Zou, T., Gao, H., Li, Y., Zhang, L., Yu, Y., Xiao, R., Wang, Y., Yi, C., Wang, Z., Shi, J., Guo, Y., Wu, Y., 2025. Polarization Calibration Verification of the Directional Polarimetric Camera on the Terrestrial Ecosystem Carbon Inventory Satellite. IEEE Transactions on Geoscience and Remote Sensing, 63, 1-12.

Zhang, P., Gu, S., Chen, L., Shang, J., Lin, M., Zhu, A., Yin, H., Wu, Q., Shou, Y., Sun, F., Xu, H., Yang, G., Wang, H., Li, L., Zhang, H., Chen, S., Lu, N., 2023a. FY-3G Satellite Instruments and Precipitation Products: First Report of China’s Fengyun Rainfall Mission In-Orbit. Journal of Remote Sensing, 3, 0097.

Zhang, Z., Fu, G., Hasekamp, O., 2023b. Aerosol retrieval over snow using the RemoTAP algorithm. Atmospheric Measurement Techniques, 16(24), 6051-6063.

Zhang, Z., Li, Z., Fu, G., Hasekamp, O., Fan, C., Qie, L., Xie, Y., Li, L., Ji, Z., Liu, Q., 2025a. Global Aerosol Retrieval Over Land Using the Chinese Satellite Polarimeter DPC-2/GF-5(02). IEEE Transactions on Geoscience and Remote Sensing, 63, 1-14.

Zhang, Z., Yan, L., Jiang, X., Zhang, F., Ding, J., XU, Y., Shang, K., Liu, Z., 2025b. Polarimetric ocean remote sensing: Classic feature analysis and novel feature establishment. Science China Earth Sciences, 68(7), 2237-2252.